Fermi National Accelerator Laboratory

Recent Results from Fermilab E690

M.C. Berisso et al.

Fermi National Accelerator Laboratory
P.O. Box 500, Batavia, Illinois 60510

January 1998

Disclaimer

This report was prepared as an account of work sponsored by an agency of the United States Government. Neither the United States Government nor any agency thereof, nor any of their employees, makes any warranty, expressed or implied, or assumes any legal liability or responsibility for the accuracy, completeness, or usefulness of any information, apparatus, product, or process disclosed, or represents that its use would not infringe privately owned rights. Reference herein to any specific commercial product, process, or service by trade name, trademark, manufacturer, or otherwise, does not necessarily constitute or imply its endorsement, recommendation, or favoring by the United States Government or any agency thereof. The views and opinions of authors expressed herein do not necessarily state or reflect those of the United States Government or any agency thereof.

Distribution

Approved for public release; further dissemination unlimited.

Recent Results from Fermilab E690

M.C. Berisso†, D.C. Christian$^\|$, J. Felix*, A. Gara‡, E. Gottschalk$^{\ddagger 1}$, G. Gutierrez$^\|$,
E.P. Hartouni$^{\dagger 2}$, B.C. Knapp‡, M.N. Kreisler†, S. Lee$^{\dagger\ 3}$, K. Markianos†,
G. Moreno*, M.A. Reyes*, M. Sosa*, M.H.L.S. Wang†, A. Wehmann$^\|$, D. Wesson$^{\dagger 4}$

**Universidad de Guanajuato, Leon, Guanajuato, Mexico,* †*University of Massachusetts,*
Amherst, Massachusetts, USA, $^\|$*Fermilab, Batavia, Illinois, USA,* ‡*Columbia University, Nevis*
Labs, New York, USA

Abstract. Partial wave analysis results of centrally produced mesons in the reaction
$pp \to p_{slow}(X)p_{fast}$, with 800 GeV/c protons incident on a liquid hydrogen target are
presented. In the reactions considered in this paper the (X) system decays into: a)
$K_s^0 K^\pm \pi^\mp$, b) $K_s K_s$, and c) $\pi^+ \pi^-$.

THE APPARATUS

The results presented here are based on an analysis of about 10% of the 5×10^9
events recorded by FNAL E690 during Fermilab's 1991 fixed target run. The E690
apparatus [1] consisted of a high rate, open geometry multiparticle spectrometer
(Figure 1) used to measure the target system (T) in $pp \to p_{fast}(T)$ reactions, and a
beam spectrometer system used to measure the incident 800 GeV/c beam and scat-
tered proton. A liquid hydrogen target was located just upstream of the multiparti-
cle spectrometer. The target was surrounded by a segmented lead-scintillator "veto
counter," which was used to detect the presence of charged or neutral particles out-
side the aperture of the multiparticle spectrometer. The 96 cell Cherenkov counter
located at the downstream end of the main spectrometer magnet used Freon 114 as
a radiator and had a pion threshold of 2.57 GeV/c. The multiparticle spectrometer
had an approximately 700 mrad geometrical acceptance, and very good momentum
resolution from 0.2 GeV/c up to about 15 GeV/c (a typical K_s peak has a FWHM
of 4 MeV/c^2, see Fig. 6.c). A time-of-flight system provided π/p separation up
to 1.5 GeV/c. The beam spectrometer had a transverse-momentum acceptance up
to 0.8 GeV/c, with a resolution of $\sigma_{p_t} = 7$ MeV/c; and a longitudinal-momentum
acceptance from 800 GeV/c down to about 600 GeV/c, with a resolution of $\sigma_{p_L} =$
400 MeV/c.

The trigger required the same number of incoming and outgoing beam tracks,
and at least one non-beam track in the multiparticle spectrometer.

So far the search for non $q\bar{q}$ mesons in the data has been done in the following
three reactions:

$^{1)}$ Present address: University of Illinois, Urbana, Illinois.
$^{2)}$ Present address: Lawrence Livermore National Laboratory, Livermore, California.
$^{3)}$ Present address: SKY Computers, Inc., Chelmsford, Massachussets.
$^{4)}$ Present address: OAO Corporation, Athens, Georgia.

$$pp \longrightarrow p_{slow}(K_s^0 K^{\pm} \pi^{\mp})p_{fast} , \qquad K_s^0 \to \pi^+ \pi^- \qquad (1)$$

$$pp \longrightarrow p_{slow}(K_s^0 K_s^0)p_{fast} , \qquad K_s^0 \to \pi^+ \pi^- \qquad (2)$$

$$pp \longrightarrow p_{slow}(\pi^+ \pi^-)p_{fast} \qquad (3)$$

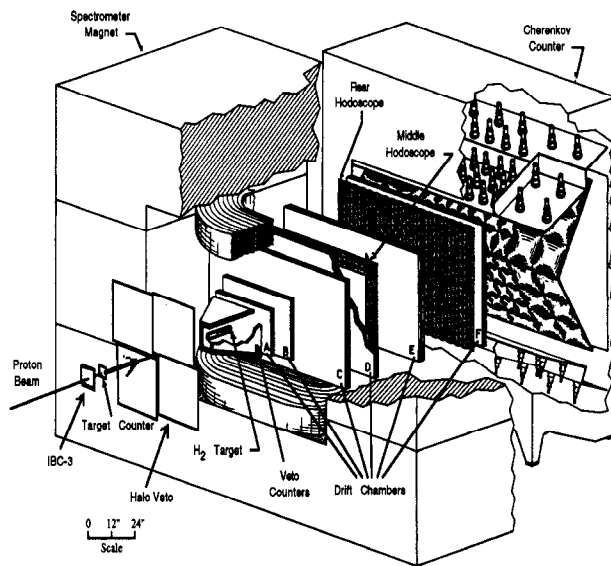The analysis results of the above reactions will be reported in this paper.

FIGURE 1. E690 Multiparticle Spectrometer.

THE COORDINATE SYSTEM

Reactions (1-3) were analyzed as a two step process: the production step in which an (X) system is formed by the collision of two objects (referred to as pomerons) emitted by the scattered protons, and the decay step, where (X) decays into either two particles (2-3), or a particle and an isobar (1), with the subsequent decay of the isobar into two particles.

The production coordinate system was defined in the center of mass of the (X) system, with the y-axis perpendicular to the plane of the two pomerons in the pp center of mass, and the z-axis in the direction of the beam pomeron in the (X) center of mass. It should be emphasized here that there is no unique way of defining the production coordinate system in central production. The direction of the pomerons in the (X) center of mass is uniquely defined, but rotations around this axis are

not. For example, the y-axis could have been defined as perpendicular to the plane formed by the beam and fast protons, or by the target and slow protons, in the (X) center of mass.

If the assumption that the (X) system is formed by the collision of two objects emitted by the scattered protons is accurate, then our selection of the y-axis is natural. A large rapidity gap between the protons and any of the central products will favor the assumption that (X) is formed by the exchange of two pomerons. In the data used for this paper the rapidity gap between p_f and the fastest central particle is at least 3.5 units, and between p_s and the slowest central particle at least 1.8 units.

The two variables needed to specify the (X) decay into two particles (2-3) were taken as the polar and azimuthal angles of one of the decay products in the production coordinate system. For the $K_s K_s$ system (2) , the K_s that defines the direction was taken at random. For the three body decay of the (X) the decay of the meson system was characterized by its isobar mass, the polar and azimuthal angles of the bachelor particle in the production coordinate system, and similar decay angles for the $K^{\pm}$ produced in the isobar decay in a coordinate system defined by a Lorentz boost from the $K\overline{K}\pi$ center of mass to the center of mass of the isobar.

The five variables used to specify the production process were the x_F and invariant mass of the (X) system, the transverse momenta of the slow and fast protons $(p_{t,s}^2, p_{t,f}^2)$, and δ, the angle between the planes of the scattered protons in the (X) CM. The analyses presented in this paper were done in bins of the (X) invariant mass, for the selected region in x_F, integrating over $p_{t,s}^2$, $p_{t,f}^2$ and δ.

No direct measurement of the slow proton p_{slow} was made in any of the three reactions (1-3). In each case, a clear proton peak was visible in the plot of the missing mass recoiling against the directly measured particles. For the selected events the proton mass was assigned to the missing momentum and the three momentum of p_{slow} and the longitudinal momentum of p_{fast} were calculated using energy and momentum conservation.

In the two step process considered here, the (X) system is formed by the interchange of two pomerons, whose momentum vectors lie in a plane in the pp center of mass system. Parity conservation in the strong interactions implies that reflection in this plane should be a symmetry of the system [12]. Therefore the amplitudes used for the partial wave analysis were defined in the reflectivity basis [2].

FINAL STATE: $P_{SLOW}(K_S^0 K^{\pm}\pi^{\mp})P_{FAST}$

This final state was selected by requiring an interaction vertex in the LH_2 target with one positive track, one negative track, and a K_s^0. At least one of the two charged tracks originating at the interaction vertex was required to be identified by the Cherenkov counter (as either a π, or ambiguous K/p), and the other one was required to be compatible with the assumed identity. No direct measurement was made of the slow proton. The missing mass squared shown in Figure 2 has a clear

proton peak for both charge states of reaction 1; this quantity was required to be between -1.0 and 2.2 $(\text{GeV}/c^2)^2$.

In all events selected by the cuts listed above, the forward proton, p_{fast}, was separated from the central mesons by at least 3.5 units of rapidity. A minimum gap of 1.8 units of rapidity was required between each individual meson and p_{slow}. The x_F of the meson system was required to be in the range $[-0.15, -0.02]$.

Figures 2.a and 2.c show the $K\overline{K}\pi$ invariant mass distributions for the selected data sample. In both charge states, the spectrum is dominated by two peaks. One of these is easily identified by its mass and width as the $f_1(1285)$. The second peak has a central value of approximately 1430 MeV/c^2. No obvious structure is seen at higher mass. In particular, the $f_1(1510)$ seen in K^-p interactions [3] is not evident.
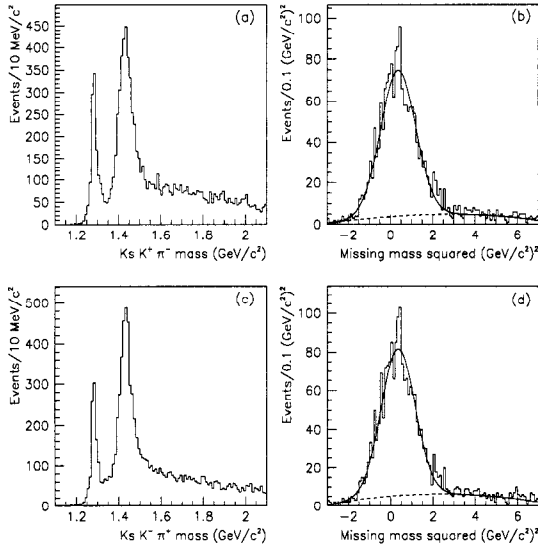

FIGURE 2. a) Invariant mass, and b) Missing mass squared between threshold and 1480 MeV/c^2 for $K_s^0 K^+\pi^-$. c) Invariant mass, and d) Missing mass squared between threshold and 1480 MeV/c^2 for $K_s^0 K^-\pi^+$.
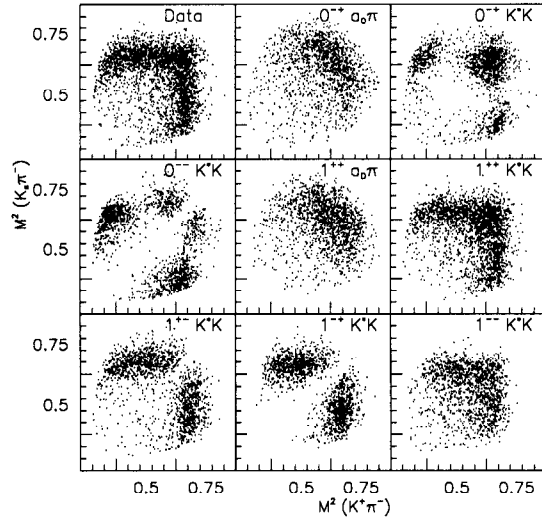
FIGURE 3. Dalitz plots for both data and MC for the $K_s^0 K^+\pi^-$ system.

Figure 3 shows the Dalitz plot for the $K_s^0 K^+\pi^-$ mass range 1390-1480 MeV/c^2. Examination of these Dalitz plots shows that the peak at 1430 MeV/c^2 is almost certainly dominated by decays of a single 1^{++} meson, the $f_1(1420)$, into the final state K^*K. The Dalitz plot labelled "Data" shows clear bands at the K^* mass, and an excess in the upper right corner. This indicates decay to K^*K, with the charged and neutral K^*'s interfering constructively, as required by even G parity.

A full Partial Wave Analysis was done using the BNL-MPS parameterization [4]. Waves were labelled with spin, parity, and G-parity J^{PG}, the isobar, and the absolute value of the spin projection and naturality $|J_z|^\eta$. All waves with spin 0 and 1 and isobars K^* and a_0 were tried. No incoherent background term was

included in the fit. The $K^*(892)$ isobar was parameterized by a relativistic Breit-Wigner function, with mass and width as listed by the Particle Data Group [5]. The parameterization given in [4] was used for the $a_0(980)$.

The wave amplitudes were determined by maximizing the log of the extended likelihood function [6]. The analysis was done in 10 MeV/c^2 bins of $K\overline{K}\pi$ mass, from threshold to 1600 MeV/c^2, for both charge states separately. The analysis for each charge states gave identical results. Only the results for $K_s^0 K^+ \pi^-$ will be shown here.

The partial wave analysis was performed for each mass bin separately. First, each of the eighteen waves were tried one at a time. The single wave which maximized the likelihood was kept, and each of the remaining seventeen waves added to it one at a time. The two wave solution which maximized the likelihood was kept for the third iteration, and each of the remaining sixteen waves added one at a time. This process of adding one wave per iteration was continued until no significant improvement in the likelihood was observed. Below 1290 MeV/c^2, only the two 1^{++} $a_0\pi$ waves with $|J_z|^\eta = 1^\pm$ (the $f_1(1285)$) were required. Above 1290 MeV/c^2, four dominant waves were found: 1^{++} K^*K $|J_z|^\eta = 1^\pm$ (the $f_1(1420)$), and 1^{+-} K^*K $|J_z|^\eta = 1^\pm$. For the $K_s^0 K^+ \pi^-$ final states the final step of this procedure is illustrated in Figure 4. In this figure, the acceptance corrected intensities (normalized to the number of events) are shown for each set of waves. In each case, one additional wave was added to the dominant waves. For spin one, the figures show a sum of the $|J_z|^\eta$ components.
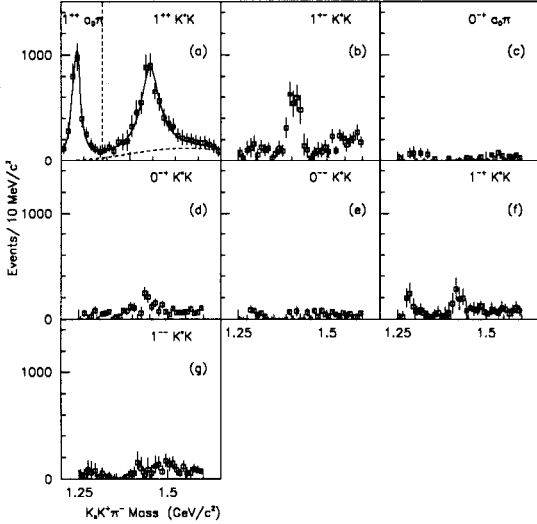

FIGURE 4. Partial wave intensities for the $K_s^0 K^+ \pi^-$ system. The waves (c) to (g) were added one at a time to the waves (a)+(b).
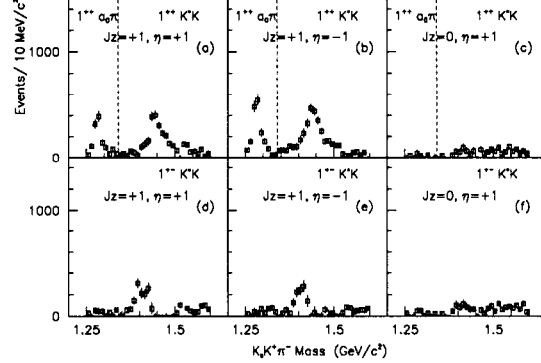
FIGURE 5. Separate $|J_z|^\eta$ partial wave intensities for the $K_s^0 K^+ \pi^-$ system.

As stated above, the data can be described completely using only waves with $|J_z|^\eta = 1^\pm$. This striking result is illustrated in Figure 5 for the $K_s^0 K^+ \pi^-$ final

states. The figure shows the intensities extracted using six waves in each mass bin. For all three states, the solution contains equal amounts of $|J_z| = 1$, $\eta = \pm 1$, and no $|J_z| = 0$. This result may be a consequence of the production mechanism [7]. If a meson of spin J is formed by the interaction of two identical particles of helicities λ_1 and λ_2, then the production amplitude $F^J_{\lambda_1 \lambda_2} = (-1)^J F^J_{\lambda_2 \lambda_1}$. Therefore $J = 1 \Rightarrow \lambda_1 \neq \lambda_2 \Rightarrow J_z = \lambda_1 - \lambda_2 \neq 0$.

The 1^{+-} K^*K state seen in the previous studies may be an artifact of the way the analysis was done. It is likely that the inclusion of the tail of $f_1(1285)$ above 1290 MeV/c^2 will make this state disappear. This problem is now under study.

FINAL STATE: $P_{SLOW}(K^0_S K^0_S)P_{FAST}$

This Final state was selected by requiring a primary vertex in the LH_2 target with two K_s, an incoming beam track, and a fast forward proton. No direct measurement of the slow proton p_{slow} was made, and no direct particle identification was used. The target veto system was used to reject events with more than a missing proton.

The missing mass squared seen in Figure 6.a shows a proton peak with little background. Figure 6.b shows the uncorrected x_F distribution for the $K_s K_s$ system. The arrows in Figures 6.a,b indicate the cuts used in the event selection. With these cuts, the minimum rapidity gap between p_{slow} and the $K_s K_s$ system is 1.2 units. The rapidity gap between the meson system and p_{fast} is greater than 3.7 units for all events.
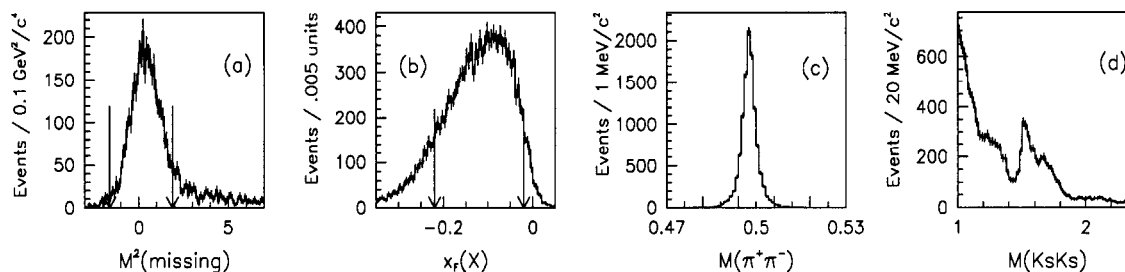

FIGURE 6. a) Missing mass squared for $1.4 < M(K_s K_s) < 1.8$ GeV/c^2. b) Uncorrected x_F distribution. c–d) Measured $\pi^+\pi^-$ and $K_s K_s$ invariant mass.

Figure 6.d shows the $K_s K_s$ invariant mass for the events that passed the previous cuts. The current analysis was performed using 11182 events with $K_s K_s$ mass between 1 and 2 GeV/c^2. For $-0.22 < x_F < -0.02$ the $K_s K_s$ invariant mass beyond 2 GeV/c^2 is smooth, with no evidence of the $\xi(2230)$ state seen by the BES Collaboration [8].

The acceptance corrected $\cos\theta$ and ϕ distributions are shown in Figures 7 and 8. The acceptance is flat in ϕ, and dips near $\cos\theta = \pm 1$. On average the correction at $\cos\theta = \pm 1$, relative to the correction at 0, is 65%.
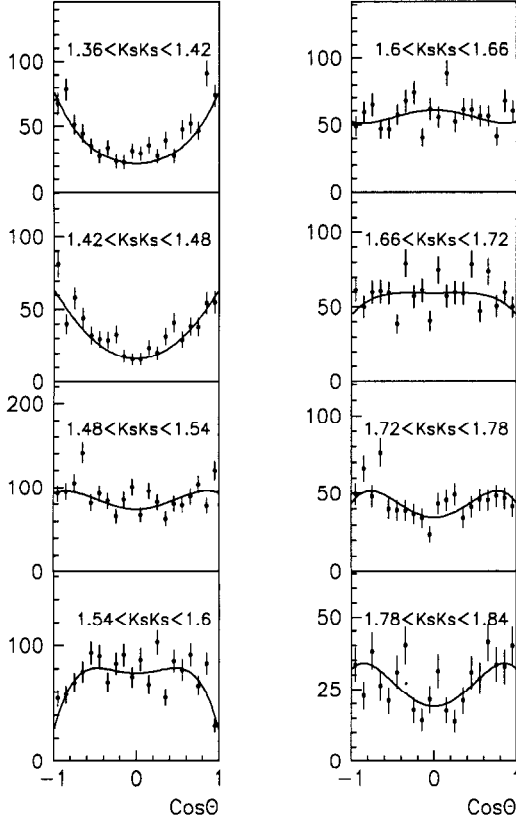
FIGURE 7. Acceptance corrected $\cos\theta$ angular distributions in bins of the $K_s K_s$ invariant mass, starting at 1.36 GeV/c² in steps of 60 MeV/c².
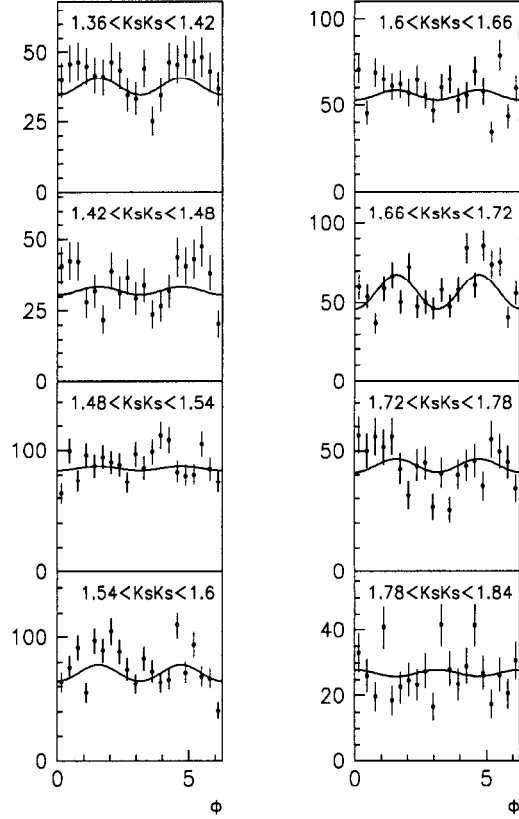
FIGURE 8. Acceptance corrected ϕ angular distributions in bins of the $K_s K_s$ invariant mass, starting at 1.36 GeV/c² in steps of 60 MeV/c².

These distributions are very different than the K^+K^- angular distributions observed by WA76 [9]. In the mass region around 1525 MeV/c² our angular distributions are fairly flat, while the WA76 K^+K^- distributions show a distinctively spin 2 pattern.

A detailed partial wave analysis was performed from threshold to 2 GeV/c². The analysis was done in two different ways. First, the amplitudes were extracted from the moments. Second, the amplitudes were determined by maximizing the extended likelihood with respect to the wave moduli and the relative phases. Within errors both analyses gave the same answer [10,11].

The inherent ambiguities of a two body system are such that in our analysis there are two solutions for each mass bin [12,13]. Both solutions give identical moments or identical values of the likelihood. In order to continue the solutions from one mass bin to the next, one follows the Barrelet zeros [12,13]. In general these zeros are complex and one lies above the real axis and the other lies below it. When the zeros cross the real axis the solutions bifurcate. In the analysis presented here, there

is a bifurcation point at 1.58 GeV/c^2. Before this bifurcation point there are two solutions, one which is mostly S wave, and another that is mostly D wave. Since at threshold the $K_s K_s$ cross section is dominated by the presence of the $f_0(980)$ [14] it is possible to eliminate the solution that has a very small S wave contribution at threshold. The remaining solution bifurcates at 1.58 GeV/c^2 into a solution that has a large S wave contribution, and another that has a large D wave component.

For the plots and details of the analysis see References [10,11].

FINAL STATE: $P_{SLOW}(\pi^+\pi^-)P_{FAST}$

This final state was selected by requiring a primary vertex in the LH_2 target with one positive track, one negative track, an incoming beam track, and a fast forward proton. The positive and negative tracks were required to be pion compatible in the Cherenkov counter.

The missing mass squared seen in Figure 9.a shows a clear proton peak. To eliminate backgrounds a tight cut $-0.56 < MM^2 < 1.12$ GeV^2/c^4 was applied. Figure 9.b shows the uncorrected x_F distribution for the selected events. Only events in the interval $-0.1 < x_F < 0$. were used in the analysis.

Rapidity gaps between p_f and the fastest central pion of at least 3.5 units, and between p_s and the slowest central pion of at least 1.8 units were required. Finally, the transverse momentum of both protons was required to be less than $p_t^2 < 0.1$ $(GeV/c)^2$.
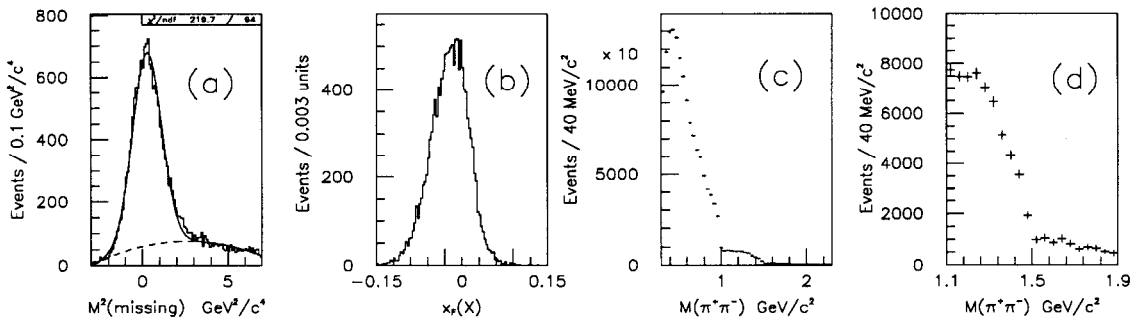

FIGURE 9. a) Missing mass squared. b) Uncorrected x_F distribution. c–d) Acceptance corrected $\pi^+\pi^-$ invariant mass.

Figures 9.c and 9.d show the acceptance corrected $\pi^+\pi^-$ invariant mass. Three striking features are observed: a) the absence of the ρ meson, b) the sudden drop at 1 GeV/c^2 due to the $f_0(980)$, and c) a second drop at about 1.45 GeV/c^2, which is most likely due to the $f_0(1500)$. Similar features have been observed before [15,9]. Double pomeron exchange (or any state formed by two identical bosons) only allows states with quantum numbers $J^{PC} = (even)^{++}$. Therefore in the limit

of large rapidity gaps between the protons and the pions, and low p_t^2, the ρ signal is expected to vanish, as is seen in our data.

To determine the spin and parity of the states present in our data a full partial wave analysis was performed from threshold to 1.6 GeV/c^2 in bins of 40 MeV/c^2 [16]. Al waves with J=0,1 and 2, and $|J_z|^\eta$=0,1$^\pm$ were considered. The projections $|J_z|^\eta$=2$^\pm$ were not considered because the moments where these projections contribute are flat.
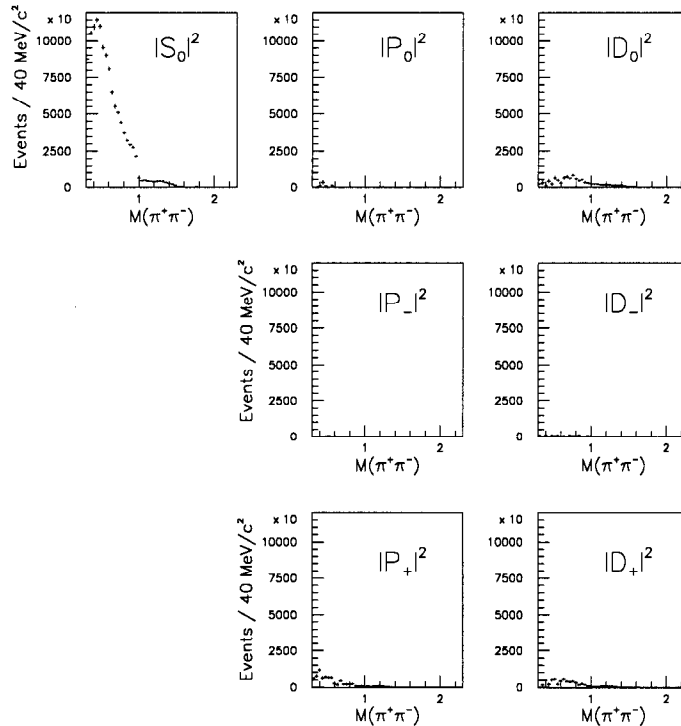

FIGURE 10. Events as a function of $\pi^+\pi^-$ invariant mass (in GeV/c^2) for different waves.

After the acceptance corrected moments were calculated, the amplitudes for each wave were extracted by inverting the relation between the moments and the amplitudes. Since this relation is non-linear the inversion yields several solutions [17]. For the waves considered here there are eight solutions for each mass bin. The connection between the solutions in one bin and the next one is done following the Barrelet zeroes [13]. In our case four zeroes have to be followed in the complex plane as a function of mass. Every time the imaginary part of one of the zeroes crosses the real axis the solution bifurcates. No crossing of the zeroes with the real axis was observed in our data; therefore it is possible to follow all eight solutions from threshold to 1.6 GeV/c^2. Near threshold the D-wave is the dominant contribution for six out of the eight solutions. Of the remaining two, one has the same amount of S-wave and D-wave near threshold. These seven solutions can be ruled

out because the $\pi^+\pi^-$ cross section near threshold is known to be dominated by S-wave [14]. The remaining solution is shown in Figure 10. It is easy to see that in this case the cross section is entirely dominated by S-wave from threshold to 1.6 GeV/c^2.

ACKNOWLEDGMENTS

REFERENCES

1. The E690 multiparticle spectrometer was previously used at the Brookhaven National Laboratory in BNL E766 and is described in Uribe, J., *et al.*, *Phys.Rev.* **D49** (1994) 4373. The beam chambers are described in Christian, D.C., *et al.*, *NIMA* **345** (1994) 62–71.
2. Chung, S.U., and Truman, T.L., *Phys.Rev.* **D11** (1975) 633.
3. Aston, D., *et al.*, *Phys.Lett.* **201B**, 573 (1988); Gavilet, P., *et al.*, *Z.Phys.* **C16**, 119 (1982).
4. Chung, S.U., "Formulas for Partial Wave Analysis", BNL Report (1989); Blessing,S.K., Ph.D. thesis, Indiana University (1988).
5. Particle Data Group, *Phys.Rev.* **D54**, 1 (1996).
6. Sosa, M., Ph.D. thesis, Universidad de Guanajuato, México (1996).
7. This explanation was suggested by S.U. Chung; Chung, S.U., CERN Yellow Report, CERN 71-8 (1971). See also F. Close contribution to these proceedings.
8. Bai, J.Z., *et al.*, *Phys.Rev.Lett.* **76** (1996) 3502.
9. Armstrong, T.A., *et al.*, *Phys.Lett.* **B227** (1989) 186, and *Z.Phys.* **C51** (1991) 351.
10. Reyes, M.A., *et al.*, *Nucl.Phys. B (Proc. Suppl.)* **56A**, (1997) 285–290.
11. Reyes, M.A., *et al.*, contribution to these proceedings.
12. Chung, S.U., BNL-QGS-94-23, and BNL-QGS-96-32.
13. Barrelet, E., *Nuovo Cimento* **A8** (1972) 331.
14. Au, K.L., Morgan, D., and Pennington, M.R., *Phys.Rev.* **D35** (1987) 1633; Morgan, D., and Pennington, M.R., *Phys.Rev.* **D48** (1993) 1185.
15. Akesson, T., *et al.*, *Nucl.Phys.* **B264** (1986) 154.
16. Markianos, K., PhD Thesis, University of Massachusetts, Amherst (UMAHEP 449), 1998.
17. Chung, S.U., BNL-QGS-95-41.